HYDROLOGICAL PROCESSES
*Hydrol. Process.* **30**, 2305–2316 (2016)
Published online 6 March 2016 in Wiley Online Library
(wileyonlinelibrary.com) DOI: 10.1002/hyp.10790

# Discontinuous headwater stream networks with stable flowheads, Salmon River basin, Idaho

John A. Whiting* and Sarah E. Godsey

*Department of Geosciences, Idaho State University, 921 South 8th Ave. Stop 8072, Pocatello, ID, 83209-8072, USA*

## Abstract:

Headwater streams expand, contract, and disconnect in response to seasonal moisture conditions or those related to individual precipitation events. The fluctuation of the surface flow extent, or active drainage network, reflects catchment storage characteristics and has important impacts on stream ecology; however, the hydrological mechanisms that drive this phenomenon are still uncertain. Here, we present field surveys of the active drainage networks of four headwater streams in Central Idaho's Frank Church-River of No Return Wilderness (7–21 $km^2$) spanning the spring and summer months of 2014. We report the total length of the active drainage networks, which varied as a power law function with stream discharge with an average exponent of $0.11 \pm 0.03$ (range of 0.05–0.20). Generally, these active drainage networks were less responsive to changes in discharge than many streams in past studies. We observed that the locations where surface flow originates, or flowheads, were often stable, and an average of 64% of the change in active drainage network length was explained by downstream discontinuities. Analysis of geologic and geomorphic characteristics of individual watersheds and flowheads suggests that most flowheads below approximately 2200 m are supported by stable flowpaths controlled by bedrock structure. At higher elevations, small accumulation areas and saturation of shallow and conductive soil and colluvium after snowmelt result in more mobile flowhead locations. The dynamics of active drainage networks can help illuminate the spatiotemporal structure of flowpaths supporting surface flow. Copyright © 2016 John Wiley & Sons, Ltd.

KEY WORDS catchment hydrology; stream network; active drainage network; headwater streams; channel head; subsurface flow

*Received 28 October 2015; Accepted 15 January 2016*

## INTRODUCTION

As surficial expressions of groundwater conditions, streams provide accessible information regarding the spatiotemporal variability of subsurface storage (Biswal and Kumar, 2013; Bencala *et al*., 2011; Kirchner, 2009). Headwater stream networks are particularly revealing as they expand and contract in response to individual precipitation events (Day, 1978, 1983) and seasonal moisture conditions (Godsey and Kirchner, 2014; Roberts and Archibold, 1978; Blyth and Rodda, 1973; Roberts and Klingeman, 1972; Gregory and Walling, 1968). Each location where flow either surfaces or infiltrates marks a point where incoming flows equal the ability of the subsurface to accommodate that flow, and the expansion and contraction of the active stream network potentially mirror the spatial extent of subsurface water availability (Godsey and Kirchner, 2014). The dynamic headwaters of streams constitute most of the channel length of all stream networks and significantly influence downstream systems (Bishop *et al*., 2008; Leopold *et al*., 1964).

Understanding catchment storage is important for managing water for human needs (e.g. Goyal *et al*., 2015), evaluating riparian and terrestrial ecosystem impacts (e.g. Jaeger *et al*., 2014; Davis *et al*., 2013), managing stream responses to wildfire (e.g. Wagner *et al*., 2014), and for comparing catchments' hydrologic response (McNamara *et al*., 2011). Complex storage characteristics of natural watersheds are often modelled in order to explain drainage behaviour. These models necessarily make important assumptions about natural systems, which may facilitate or obscure key processes. For example, Kirchner (2009) proposes a rainfall–runoff model based on the assumption that the drainage characteristics of a single storage–discharge relationship can explain streamflow at the catchment-scale. Additionally, Biswal and Marani (2010) propose a geomorphological recession flow model, which assumes drainage of an unconfined aquifer by an intersecting channel network. Furthermore, a given length of stream in this conceptualized network maintains the same discharge throughout the entire network, and thus, the rate of stream length recession remains constant (Biswal and Marani, 2010;

*Correspondence to: John A. Whiting, Department of Geosciences, Idaho State University, 921 South 8th Ave. Stop 8072, Pocatello, ID 83209-8072, USA.
E-mail: jwhiting860@gmail.com

Biswal and Kumar, 2013). Such simplifying assumptions are a necessary and useful element in models; however, field validation of their accuracy and general applicability remains critical.

Quantifying watershed-scale storage characteristics is difficult, largely because of the distribution and heterogeneity of storage within snowpacks, vegetation, surface water, and especially soil moisture and groundwater (McNamara *et al.*, 2011). In particular, flows between soils and bedrock at large scales are difficult to measure accurately (e.g. Gabrielli *et al.*, 2012). However, the active stream network provides a spatially extensive reflection of groundwater conditions and hydrological processes regulating surface flow throughout a catchment. Observations of the active stream network structure and fluctuations may therefore provide useful information such as whether networks fluctuate in a consistent and connected manner as required for Biswal and Marani's (2010) model, a dynamic and disconnected fashion as described by Godsey and Kirchner (2014), or fluctuate relatively little.

Here we present field data documenting the contraction and disconnection of active drainage networks from May through August 2014 in four mountainous headwater catchments. In contrast to Godsey and Kirchner (2014), these data show more stable active drainage network dynamics with simultaneous reductions in outlet discharge. We discuss potential geologic, geomorphic, and climatic controls resulting in more stable active drainage configurations. We also assess potential controls of individual flowhead stability. Because of the general stability of the observed active drainage networks, we consider the role of groundwater, bedrock fracture flow paths, and springs as an important source of streamflow.

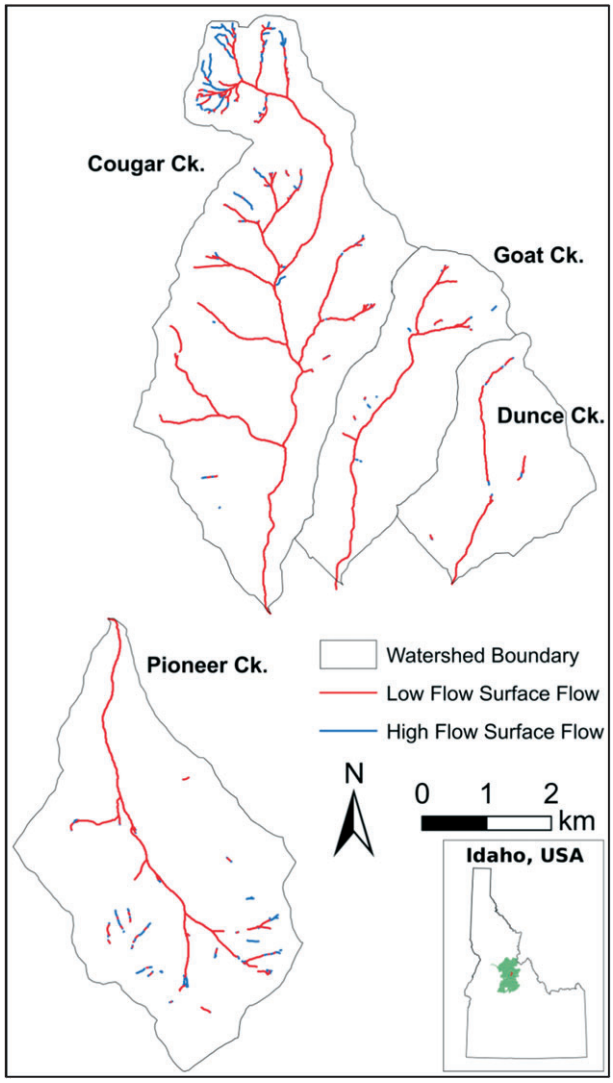


Figure 1. Surface flow mapped during the low flow surveys (18 July 2014 to 3 August 2014) in red overlies surface flow mapped during the high flow surveys (28 May 2014 to 15 June 2014) in blue. The lack of visible blue lines on the map indicates that the active stream length did not fluctuate extensively during late May to early August 2014. The inset map of Idaho, USA, includes the extent of the Frank Church – River of No Return Wilderness in green and the four study watersheds in red

## STUDY AREA AND METHODS

### *Big Creek watershed*

Big Creek is a major tributary of the Middle Fork of the Salmon River in central Idaho and flows through the Frank Church-River of No Return Wilderness. At the confluence with the Middle Fork of the Salmon River, Big Creek watershed is 1540 km$^2$ with an elevation range from 1030 to 2900 m (US Geological Survey, 2014) (Figure 1). Basin-wide mean annual precipitation is 70 cm, which primarily falls as snow in wet winter months, resulting in peak runoff from late spring to midsummer (US Geological Survey, 2014; Knowles *et al.*, 2006; Stewart *et al.*, 2004).

We observed patchy forest cover of primarily Douglas fir (*Pseudotsuga menziesii* var. *glauca*) and Ponderosa pine (*Pinus ponderosa*) with interspersed bunchgrasses, wildflowers, and occasionally sagebrush (*Artemisia*) on low-elevation hillslopes. Higher-elevation slopes are more forested with Douglas fir, and sub-alpine conifers at the highest elevations. Stands of Lodgepole pine (*Pinus contorta* var. *latifolia*) dominate some slopes recovering from wildfires.

The bedrock geology consists of the Mesoproterozoic Lemhi and Neoproterozoic Windemere Supergroups, the Eocene Challis Volcanic Group, and series of Neoproterozoic, Cretaceous, and Eocene intrusive rocks (Stewart *et al.*, 2013). Primarily northeast–southwest normal faulting is because of Neoproterozoic, Cretaceous, and Eocene extension (Stewart *et al.*, 2013). Steep hillslopes and deeply incised river canyons result from significant Neogene uplift (~10 Ma) and the related capture of the Salmon River drainage by the Snake River

(~2–4 Ma) (Sweetkind and Blackwell, 1989; Meyer and Leidecker, 1999; Kirchner et al., 2001). Steep slopes (averaging ~25°) result in thin or absent soil cover, and erosion processes are dominated by rock fall and debris flows initiated from deep-seated rotational slumps (Link *et al*., 2014).

There is clear evidence of Pleistocene alpine glaciation in the mountains of central Idaho surrounding Big Creek (Thackray *et al.*, 2004; Colman and Pierce, 1986; Dingler and Breckenridge, 1982; Evenson *et al.*, 1982; Weis *et al*., 1972), although there are no studies documenting the glacial history of Big Creek watershed. Approximately 50 km to the north, Weis *et al*. (1972) interpreted that north and northwest facing slopes higher than approximately 2440 m supported glaciers during late Pleistocene age. Just over 100 km to the south in the Sawtooth Mountains, Lundeen (2001) calculated glacial accumulation areas extending above approximately 2400 m. Additionally, Thackray *et al*. (2004) propose late Pleistocene glacial advances in the Sawtooth Mountains at approximately 14 000 years before present (YBP), and the most extensive advance around 16 900 YBP.

This study focuses on four tributaries to the lower reaches of Big Creek: Pioneer, Cougar, Goat, and Dunce Creeks (Figure 1). Pioneer Creek has a predominantly north-facing aspect, while the other three tributaries are on the north side of Big Creek and have a predominantly south-facing aspect. Pioneer and Cougar watersheds are the largest (15.8 and 21.4 $km^2$ respectively) and have the greatest elevation range (approximately 1200 to 2800 m, and 1200 to 2600 m respectively). Goat and Dunce watersheds are 7.9 and 6.5 $km^2$ respectively, and both span elevations from approximately 1100 to 2500 m (Table I).

The Frank Church-River of No Return Wilderness is the largest designated wilderness in the contiguous USA and has undergone minimal human disturbance. Because of the lack of dams, irrigation, or man-made impermeable surfaces, this is an ideal setting to study catchment hydrology. Although its headwaters are remote, the Salmon River is a major tributary to the Snake and Columbia Rivers, which act together as an important waterway for inland transport of goods to the Pacific Northwest, as well as a significant source of water and electric power to the region. This research is based at Taylor Wilderness Research Station ('Taylor Ranch'), a small facility along Big Creek owned by the University of Idaho.

### *Surface network mapping*

We mapped the extent of visible surface flow within Pioneer, Cougar, Goat, and Dunce watersheds at three times within the late spring and summer field season: a high-flow survey (28 May 2014 to 15 June 2014), intermediate-flow survey (25 June 2014 to 9 July 2014), and low-flow survey (18 July 2014 to 3 August 2014). These surveys of the watershed flow network determine the spatial distribution of surface water for a given discharge as measured at the stream outlet. While hiking throughout the respective watersheds, we used a Trimble 6000 GeoXH mapping-grade Global Positioning System (GPS) with sub-meter accuracy to manually track the locations along stream channels where surface flow begins or disappears into the subsurface. We required segments of stream flow and breaks in stream flow to be at least 20 m in length to be mapped. Pioneer and Cougar Creek watersheds span over 15 $km^2$ of rugged terrain and required at least three days to map, over which time small precipitation events sometimes

Table I. Lower Big Creek tributary characteristics and 2014 survey data

| Big Creek tributary | Watershed area ($km^2$) | Watershed altitude (m) | Survey date(s) | Average discharge ($m^3/s$) | ADN length (km) | Drainage density ($km/km^2$) | $\beta$ |
|---|---|---|---|---|---|---|---|
| Pioneer | 15.8 | 1200–2800 | 28–31 May | 0.404 ± 0.022 | 15.234 ± 0.363 | 0.97 | 0.197 ± 0.037 |
| | | | 25–27 June | 0.163 ± 0.008 | 13.129 ± 0.320 | 0.83 | |
| | | | 18–20 July | 0.127 ± 0.006 | 11.960 ± 0.296 | 0.76 | |
| Cougar | 21.4 | 1200–2600 | 6–10 June | 0.462 ± 0.016 | 39.177 ± 0.879 | 1.83 | 0.083 ± 0.10 |
| | | | 4–6 July | 0.087 ± 0.003 | 33.402 ± 0.761 | 1.56 | |
| | | | 1–3 August | 0.032 ± 0.001 | 31.470 ± 0.721 | 1.47 | |
| Goat | 7.9 | 1100–2500 | 19–20 June | 0.018 ± 0.001 | 8.319 ± 0.219 | 1.06 | 0.055 ± 0.024 |
| | | | 9 July | 0.012 ± 0.001 | 8.002 ± 0.212 | 1.02 | |
| | | | 27 July | 0.008 ± 0.001 | 7.949 ± 0.211 | 1.01 | |
| Dunce | 6.5 | 1100–2500 | 15 June | 0.025 ± 0.002 | 4.422 ± 0.122 | 0.68 | 0.093 ± 0.013 |
| | | | 8 July | 0.013 ± 0.001 | 4.117 ± 0.116 | 0.64 | |
| | | | 26 July | 0.009 ± 0.001 | 4.028 ± 0.113 | 0.62 | |

ADN length refers to the active drainage network length, defined as all surface flow from the confluence with Big Creek to all flowheads shown in Figure 1, including those separated by dry reaches from downstream surface flow. $\beta$ is the best estimate of the power law exponent of the discharge–ADN length relationship based on all survey dates. All reported uncertainties are ±1 standard error.

occurred that may have minimally affected mapping; mapping was not conducted during large precipitation events.

We processed the surface flow spatial data and maps using Environmental Systems Research Institute's ArcGIS 10.2 software. The raw dataset from mapping surface flow in the field consists of two sets of GPS points: one set represents the 'start' points of initiation of surface flow in a stream channel and the other set represents the 'end' points where surface flow ceases downstream. We delineated the channel networks using a 10 m digital elevation model (DEM) of the watersheds and the flow accumulation tool with a threshold of 50 000 $m^2$. We then used this channel network and surveyed the start/stop points to identify only the flowing channels to create the map of the surface flow networks. Because the initial DEM-based channel delineation was occasionally incorrect, especially in the headwaters where channels are smaller, we manually shifted sections of the delineated channel network to follow areas where riparian vegetation was distinguishable with the National Agriculture Imagery Program aerial photography and ensured that they intersected with mapped start and stop points.

We estimated the error associated with calculating the length of the surface flow network because of (1) differences in stream length based on National Agriculture Imagery Program imagery and the delineated stream network from the 10 m DEM, (2) an assumed 2 m uncertainty associated with each GPS point based on the scatter of points taken at a single location, and (3) an assumed 2% error because of our threshold of mapping stream segments and breaks greater than 20 m long.

*Partitioning active stream length fluctuation*. A flowhead is the first location from the top of a hillslope where surface flow initiates. Partitioning fluctuations in active stream length because of movement of the flowhead *versus* downstream fluctuations in continuity provides further insight into how stream length is changing and how water interacts with the ground surface. We calculated stream length changes resulting from stream discontinuity by first measuring the distance between flowhead locations between each of the three surface flow surveys, ΔFH. We then summed the distances between flowheads between surveys and subtracted this sum from the total fluctuation in active stream length ΔASL to calculate the total stream length changes because of stream discontinuity ΔD.

$$\Delta D = \Delta \mathrm{ASL} - \left(\sum \Delta FH\right) \tag{1}$$

*Flowhead stability*. The spatial stability of flowheads depends in part on the origins and flowpaths of the water supporting the flowhead. We quantify individual flowhead stability by calculating the difference in the flowhead accumulation area (i.e. surface area that drains to a point) between the high-flow mapping survey in late May to early June 2014 and low-flow survey in late July to early August. The difference in flowhead accumulation area (ΔfhAA) is then divided by the accumulation area of the stream network junction (*jAA*) immediately downslope of the flowhead location from the low flow survey. This last step calculates the fractional gain in flowhead accumulation area and normalizes flowhead stability to permit comparisons across different branches and watersheds.

$$\textit{normalized flowhead stability} = \frac{\Delta \mathrm{fhAA}}{jAA} \tag{2}$$

To determine flowhead accumulation area, we used the same flow accumulation tool and 10 m DEM as used for channel network delineation. As previously mentioned, mapped surface flow start and stop points did not always fall on the delineated stream network. To estimate flowhead accumulation area accurately, we manually shifted the flowheads to the closest delineated channel network.

*Measuring discharge*

We measured discharge at the base of Pioneer, Cougar, Goat, and Dunce Creeks using a SonTek Flowtracker Acoustic Doppler Velocimeter 1–2 days before and after mapping. We averaged the discharge measured before and after the respective survey and normalized by basin area for all runoff calculations reported in the succeeding text. Flows before and after each survey changed by 20% on average and by less than 60% in all cases.

We modelled the 2014 Pioneer Creek hydrograph using the relationship between the Pioneer Creek hydrograph from the past four years (Crosby *et al*., unpublished data) and US Geological Survey records from five surrounding gaging stations: Thompson Creek (13297330), Blackbird Creek (13306336), Johnson Creek (13313000), Meadow Creek (13310850), and the Middle Fork Salmon (13310199). The Pioneer Creek hydrograph from previous years was prepared using methods from Tennant *et al.*(2015). We used the SAS Institute's JMP 11 to develop a standard least squares multiple linear regression model with an $R^2$ of 0.86 and Akaike information criterion of -78006.3.

$$\begin{aligned}\mathrm{Pioneer\,CK.\,Q}\left(\mathrm{m}^3/s\right) = {} & \mathrm{a} + \mathrm{Corrected\ \ Blackbird\,Ck.\,Q} \\ & + \mathrm{Corrected\ \ Meadow\,Ck.\,Q} \\ & + \mathrm{Corrected\ Johnson\,Ck.\,Q} \\ & + \mathrm{Corrected\ Middle\ Fork\ Salmon\ Q} \\ & + \mathrm{Corrected\ Thompson\,Ck.\,Q}\end{aligned} \tag{3}$$

Corrected discharge measurements in Equation 3 (e.g. Corrected Blackbird Ck. Q) are the US Geological Survey measured discharge measurements multiplied by the modelled correction factor. Correction factors and the pre-factor $a$ for the best-fit model are summarized in Table II.

## RESULTS AND DISCUSSION

### *Stream length to discharge relationships*

The average drainage density (km/km$^2$) (Table I) decreased by a factor of 1.16 ± 0.06 between the high-flow surveys (28 May 2014 to 15 June 2014) and the low-flow surveys (18 July 2014 to 3 August 2014) conducted at Pioneer, Cougar, Goat, and Dunce Creeks. These results indicate that the active stream length fluctuated little between late May and early August 2014 (Figure 1). Stream discharge, however, decreased by a factor of approximately 3.18, 14.53, 2.28, and 2.80 at Pioneer, Cougar, Goat, and Dunce Creeks respectively. We plot total stream length as power functions of runoff with log-log slopes, $\beta$ (Figure 2). Previous studies of active network fluctuations with discharge have reported clear power law relationships ($\beta$) (e.g. Gregory and Walling, 1968; and other works summarized by Godsey and Kirchner (2014)). $\beta$ values from three lower Big Creek tributaries are significantly smaller than the average $\beta$ of 0.234 ± 0.028 from the studies summarized by Godsey and Kirchner (2014) (Figure 2). Only Pioneer watershed has a similar $\beta$ value.

Active stream lengths of the lower Big Creek tributaries are overall not as responsive to changes in discharge compared with the average stream, assuming that past network studies are representative of global headwaters. However, the distribution of $\beta$ across all sites is positively skewed, indicating that like the Big Creek tributaries studied here, many other previously studied streams are relatively unresponsive to changes in discharge (Figure 3).

Table II. Correction factors for the Pioneer Creek multiple linear regression model where X represents the flow at the specified gage location

| USGS gage location or constant | | Correction factor |
|---|---|---|
| a | | 0.016 |
| Blackbird Ck. (13306336) | If intact | 0.054*X |
| | If missing | 0.0212 |
| Meadow Ck. (13310850) | If intact | −0.174*X |
| | If missing | −0.0144 |
| Johnson Ck. (13313000) | | 0.003*X |
| Middle Fork Salmon (13310199) | | 0.001*X |
| Thompson Ck. (13297330) | | −0.094*X |

Refer to Equation 3 in text for details.

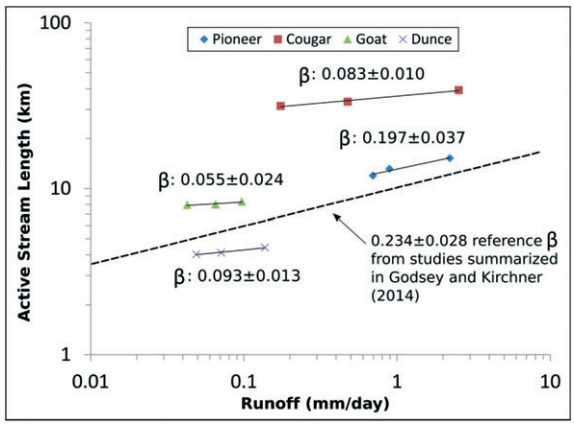


Figure 2. Active stream length (km) is plotted against runoff (mm/day) in log-log space. $\beta$ (exponent of the power law relationship) and standard error values for each of the lower Big Creek tributaries are labelled. All of the lower Big Creek tributaries have smaller $\beta$ values than the average calculated from studies summarized in Godsey and Kirchner (2014). Active stream lengths at Big Creek are therefore less responsive to changes in runoff than the average. The error associated with each measurement of active stream length is the same or smaller than the size of the point plotted above

### *Geologic and geomorphic influence on surface flow extent*

*Geology and springs*. Active stream length might be insensitive to changes in discharge for a variety of reasons, including networks being primarily spring-fed. In the field, we observed and mapped many spatially

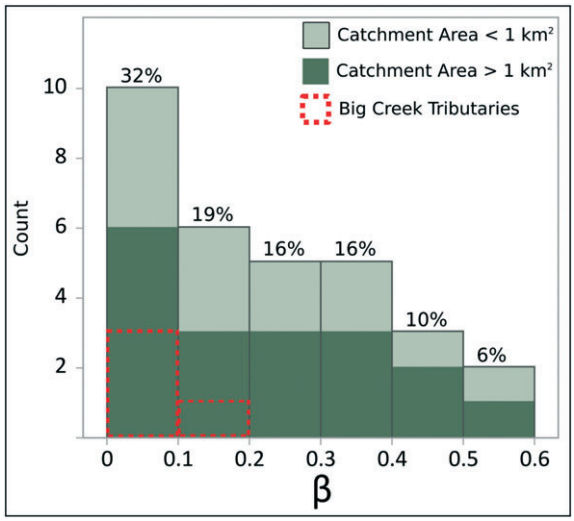


Figure 3. The distribution of $\beta$ from the lower Big Creek tributaries of this study and the 27 other sites summarized in Godsey and Kirchner (2014). The studies from catchments less than 1 km$^2$ are colored light green, while the studies from catchments greater than 1 km$^2$ are colored dark green. The distribution of catchments above and below 1 km$^2$ in area exhibit similar patterns of $\beta$. Additionally, the lower Big Creek tributaries plot on the positively skewed end of the histogram, meaning other streams are also relatively unresponsive to changes in runoff

stable spring locations where surface flow initiated. Spring discharge often became less vigorous throughout the season, but the spring location remained the same. Approximately 61%, 51%, 53%, and 91% of the changes in stream length between the high-flow and low-flow surveys were because of discontinuities in surface flow at Pioneer, Cougar, Goat, and Dunce Creeks, as opposed to downslope migration of the initial surface flow expression. Similar anchoring by springs, or seeps, was observed by Shaw (2015).

It is likely that the locations of many springs within the lower Big Creek tributaries are primarily controlled by bedrock features (e.g. joints, faults, and contacts). For example, flowheads align approximately with mapped geologic contacts of intrusive dikes in Cougar and Goat watersheds and mapped normal faults in Pioneer and Cougar watersheds (Figure 4). Other flowheads that do not align with mapped features may be associated with bedrock features of a smaller, unmapped scale or unknown subsurface structures. We present a conceptual model showing possible stream network end members: a stable spring emerging from a bedrock feature into thin overlying sediment would produce a more stable surface flow network than a stream network sourced primarily by shallow soil and regolith layers (Figure 5). In Figure 5A, the spring emerges at the approximate intersection of the controlling bedrock feature with the surface. Surface flow occurs where channel water depth is greater than the depth of the alluvial or colluvial layer overlying less conductive bedrock. In Figure 5B, surface flow begins only where the channel surface intersects the shallow soil/colluvium layer that remains above field capacity and is subject to changing locations as this layer drains or fills.

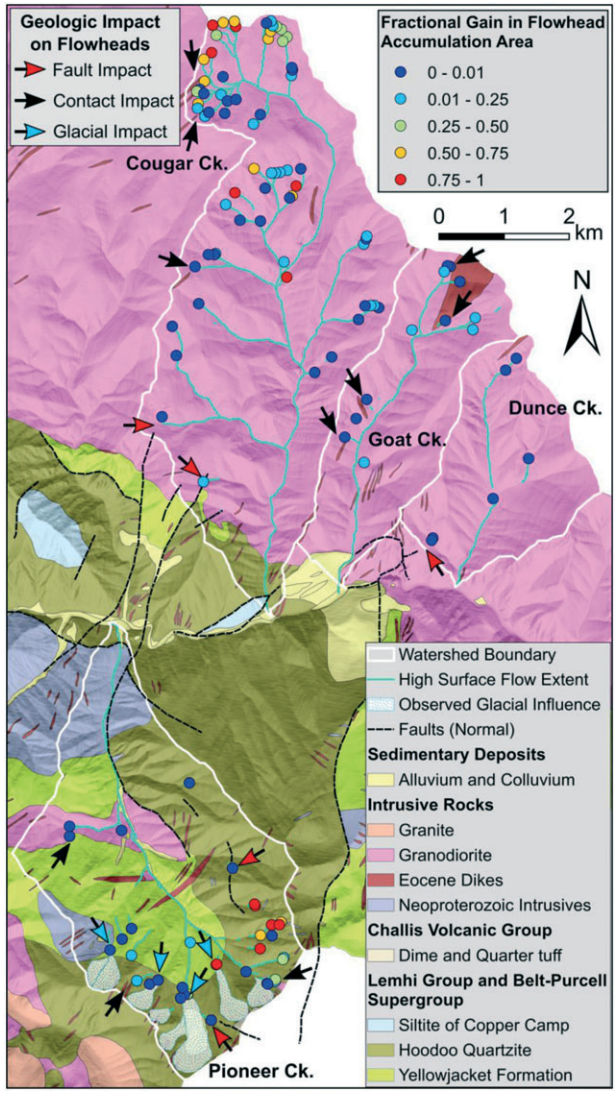


Figure 4. The bedrock geology of lower Big Creek by Stewart *et al.* (2013), overlain by locations with observed glacial influence, the high-flow active stream network and flowheads. Flowheads are colour-coded based on their spatial stability with more stable flowheads in blue and less stable in red. Arrows indicate examples of flowheads likely influenced by mapped faults (red), geologic contacts (black), or glacial geomorphology (blue)

*Accumulation area, local hillslope concavity and flowhead stability.* The two end-member controls on stream stability in Figure 5 could lead to distinct patterns of flow persistence: Figure 5A would be more stable than Figure 5B. We quantify the spatial stability of the initial surface flow expression, or flowheads, within the lower Big Creek tributaries. The stability of flowheads indicates the stability of the subsurface water source, and more stable sources are likely because of slow, long, and deep flowpaths (Figure 6A), potentially through saturated bedrock fracture networks (Figure 5A). We hypothesize that flowheads with larger accumulation areas (based on surface topography) during the high-flow survey will be more stable because longer, deeper, and slower flow paths support these locations. That is, at these locations, there is more likely to be a larger bedrock aquifer contribution to flow than at flowheads with a smaller accumulation area (Figure 6).

Accumulation areas will increase with distance from ridgelines as well as with greater hillslope concavity. Thus, we hypothesize that stable flowheads will also be in more concave regions where flowpaths converge, while unstable flowheads will be on more planar slopes where flowpaths are more likely parallel to each other. We calculated curvature perpendicular to the channel (i.e. plan curvature) at each flowhead using the ArcGIS curvature tool and the 10 m DEM used for previous analyses. Because this calculation involves the DEM cell of the flowhead and the immediately adjacent cells, curvature perpendicular to the channel was measured across approximately 30 m. Thus, curvature is measured over a distance greater than any channel width encountered; instead, the channel and at least 10 m of hillslope on either side of the channel are incorporated. Concave

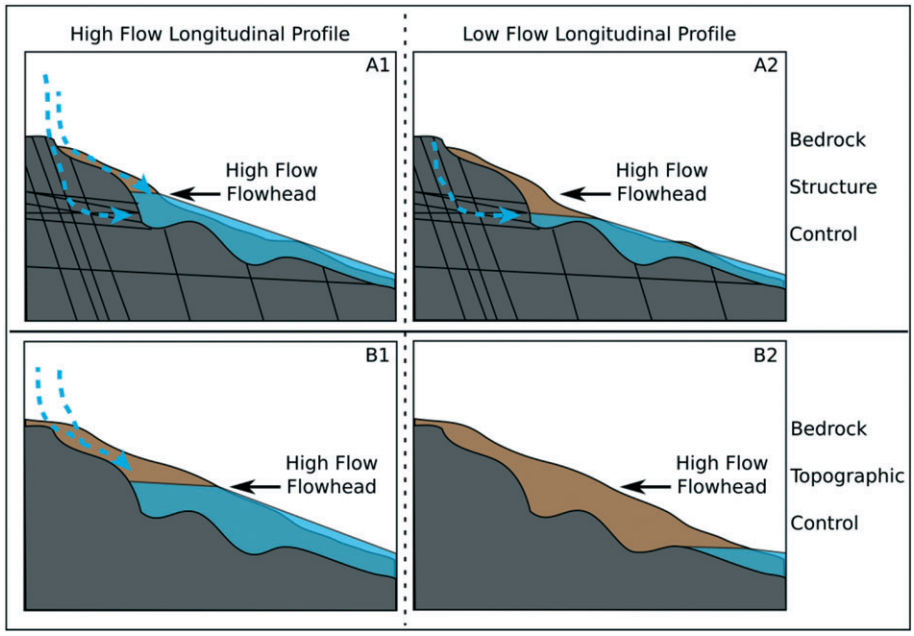


Figure 5. This conceptual model illustrates two end-member controls on stream stability. (A) Streams are likely to be more stable when supplied by deeper bedrock aquifers via stable spring locations where conductive bedrock features (e.g. joints, faults, and contacts) meet the surface. (B) Streams are likely to be less stable when supported primarily by shallow soil/colluvium layers

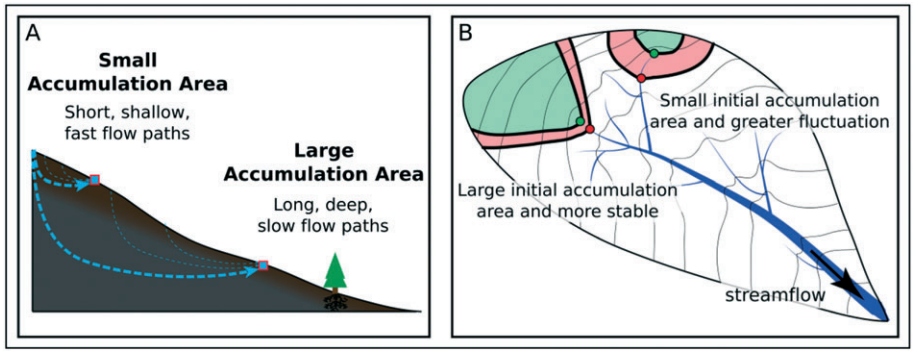


Figure 6. (A) Flowheads with small accumulation areas are supported by short, shallow, and fast flow paths, while flowheads with large accumulation areas are supported by long, deep, and slow flow paths. (B) Therefore, flowheads with large initial accumulation areas should be more spatially stable than those flowheads with small initial accumulation areas

slopes will have negative curvature values, while convex features have positive curvature values (Figure 7).

In Figure 7, the relationship between accumulation area, hillslope plan curvature, and flowhead stability becomes apparent. Flowheads with accumulation areas less than approximately 800 $m^2$ are all on nearly planar hillslopes, and 84.6% of the these flowheads are unstable (i.e. >0.25 fractional gain in flowhead accumulation area). This contrasts with flowheads with accumulation areas greater than 800 $m^2$, of which 76.3% are on concave hillslopes (i.e. < -0.4 plan curvature) and 87.8% are stable (Figure 7). These results suggest that hillslope concavities, and thus significant converging flowpaths, do not occur until flow accumulation areas greater then 800 $m^2$ are attained and stable flowheads can be supported. Furthermore, stable flowheads make up 72.6% of all flowheads, emphasizing the importance of bedrock aquifer contributions via converging, long, deep, and slow flowpaths.

Approximately 34.7% of the flowheads do not comply with the hypotheses previously mentioned. Stable flowheads in the top right quadrant of Figure 7 are supported by large accumulation areas but are on relatively planar slopes. These flowheads may be in wider valleys where the 30 m cross section considered by the planar curvature tool does not account for the overall shape of the accumulation area. More puzzling, however, are the unstable flowheads on concave slopes with large accumulation areas. These flowheads are on steep slopes at high

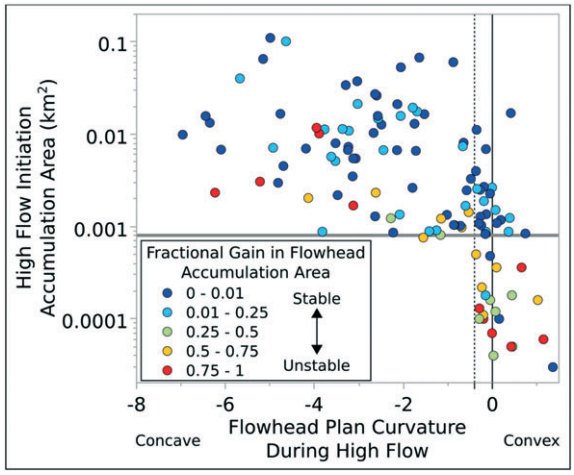


Figure 7. Fractional gain in flowhead accumulation area is a measure of flowhead stability [refer to Equation 2 in text]. Flowheads that do not move will have a value of zero (dark blue), while flowheads to stream branches that disappear completely will have a value of one (red). Flowhead plan curvature is measured perpendicular to flow using a 10 m resolution DEM, which was also used to determine accumulation area. Points to the right of the vertical dotted line (−0.4 curvature) are on approximately planar hillslopes. The gray horizontal line marks 800 $m^2$ of accumulation area, below which flowheads are on planar slopes and 84.6% of flowheads are unstable (i.e. >0.25 fractional gain in flowhead accumulation area). Flowheads ( 78.2%) have accumulation areas greater than 800 $m^2$, and 87.8% of those flowheads are stable. The unstable flowheads on concave hillslopes are likely on steep rockfall and avalanche paths with little storage capability

elevations and are thus likely within avalanche and rock fall paths with very thin soil and debris layers that rapidly release infiltrated snowmelt. Finally, the four stable flowheads on planar slopes with small accumulation areas may have more stable sources despite a small surface accumulation area. That is, bedrock features controlling the spring location and flow may not be well reflected by surface topography. This is consistent with previous studies that suggest that surface topography is not the best predictor of hillslope moisture conditions (Shaw, 2015; Gannon *et al*., 2014; Zimmer *et al*., 2013; Tromp-Van Meerveld and McDonnell, 2006; Buttle *et al.*, 2004; Freer *et al*., 2002).

To further test whether flowhead stability can provide an accurate estimate of supporting flowpath characteristics, we need to better assess the source waters of the springs and other flow initiation points throughout these watersheds. Isotopic and other chemical analyses of water samples from these locations would provide valuable information on the water's origins, and flowpath similarly to studies like Mueller et al. (2014), Liu *et al*. (2013), and Zimmer *et al*. (2013). Geophysical data similar to that collected by Daesslé *et al*. (2014) and Bièvre *et al*. (2012) or a network of wells penetrating into the bedrock immediately upslope of flow initiation points would provide a more direct view of the subsurface and potential flowpaths.

*Elevation, aspect and flowhead stability.* Flowhead stability also appears to be influenced by elevation and aspect. Flowhead stability depends on (1) the timing of snowmelt, subsurface storage, and drainage throughout the watershed and (2) geomorphology and near-surface hydrogeology, which impact the structure of aquifers and flow throughout the watershed. Approximately 88% of unstable flowheads (>0.25 fractional change) are above 2200 m. This is probably because of the influence of snowmelt and small accumulation areas. During the beginning of the surveys in late May, the snowline was around 2000 m and quickly retreating upslope. Thus, flowheads may have been at higher locations during the short period when surrounding soils and colluvium were saturated. Because lower-elevation snowpacks are smaller and melt multiple times throughout the winter, spring snowmelt at lower elevations has a limited effect on flowhead extent. Less than 14% of Goat and Dunce watersheds are above 2200 m, compared with greater than 26% of Pioneer and Cougar watersheds, and thus exhibit much more stable flowheads compared with flowheads at higher elevations within Pioneer and Cougar watersheds. This is consistent with long-term isotopic analysis from springs suggesting that as snowpacks diminish water becomes increasingly older (Manning *et al*., 2012; Rademacher *et al*., 2005), and thus rain-dominated catchments should rely on long and deep flowpaths to support stable flowheads.

In Pioneer watershed, less stable flowheads are on high west-facing slopes, compared with the more stable flowheads on the high northeast-facing slopes (Figure 4). Aspect likely influenced glacial history, and thus, present-day surface hydrology as well. High, northeast-facing slopes are the most sheltered from solar radiation and therefore sustain larger and longer-lived snowpacks. In these locations, we observed glacial features such as bowl-shaped cirques and moraines (Figure 4), which are consistent with studies describing glacial features in the mountains surrounding Big Creek (Thackray *et al*., 2004; Colman and Pierce, 1986; Dingler and Breckenridge, 1982; Evenson *et al.*, 1982; Weis *et al*., 1972). Bare rock on steep cirque walls does not support enough storage to sustain flow, and the highly conductive debris collected in the bottoms of cirques allows for rapid infiltration of meltwater. This meltwater resurfaces downslope at more stable locations below terminal moraines, where the thickness of debris diminishes. There is no evidence of glaciation on Pioneer watershed's steep west-facing slopes, likely a result of greater solar radiation exposure than the northeast-facing slopes at similar elevations. The lack of glacial cover on these slopes has allowed for the development of a more substantial, albeit thin, soil/colluvium layer. This thin layer supports ephemeral subsurface storage of snowmelt leading to less stable flowheads.

It is likely that the small cirque glaciers observed in the Pioneer watershed belonged primarily to the locally extensive glacial advance at approximately 16 900 YBP observed in the nearby Sawtooth Mountains (Thackray *et al*., 2004). The glacial history of Big Creek and classification of these features certainly deserve more attention.

In Cougar watershed, aspect also influences the timing of snowmelt and flowhead stability (Figure 8). In early June, there was still snow at the highest elevations, with rapid melt observed on the south-facing slopes. By the mid-June survey, snow was melting rapidly throughout the upper Cougar watershed, and it was largely gone by the early August survey. The timing of these surveys may have led to the south-facing high-elevation flowheads to appear less stable than the north-facing high-elevation flowheads (Figure 8), simply because the north-facing slopes did not have as much time to drain following primary snowmelt. Aspect may additionally impact freeze-thaw conditions that can influence near-surface bedrock fracturing. Thus, decreased weathering on more south-facing slopes may result in a thinner and less developed soil/regolith layer which drains snowmelt faster (Hinckley *et al*., 2014; Anderson *et al*., 2013; Lifton *et al*., 2009).

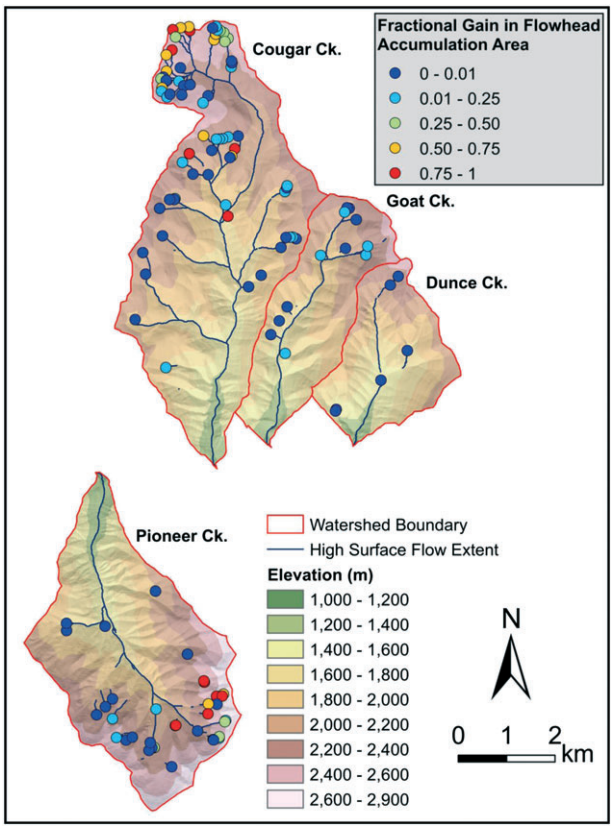


Figure 8. A topographic map of the studied watersheds, overlain by the high-flow active stream network and flowheads. Flowheads are colour-coded based on their spatial stability [Equation 2]. Flowheads at lower elevations are generally more stable than those at higher elevations. High-elevation flowheads on south- or southwest-facing slopes tend to be less stable than those on north-facing slopes

*Geology and stream length fluctuations*. The power law exponents of the active stream length–discharge relationships of Cougar, Goat, and Dunce Creeks are smaller than the average of other streams surveyed (Godsey and Kirchner, 2014). This is most likely because of the presence of stable springs controlled by fixed bedrock features (Figure 4), and the proportionately small influence of the thin, and highly conductive shallow soil layers that overlie bedrock on steep slopes. Among the lower Big Creek tributaries, only Pioneer watershed has a stream length–runoff power law exponent, or $\beta$ value, similar to that of the average $0.234 \pm 0.028$ value of streams summarized in Godsey and Kirchner (2014) (Figure 2). Pioneer watershed differs in geology and geomorphology compared with the other three tributaries. All of the lower Big Creek tributaries have primarily stable spring locations throughout their watersheds. However, Pioneer watershed has large discontinuities in surface flow, which distinguishes it from the other Big Creek tributaries. Pioneer watershed exhibits surface flow at locations with high elevations and small accumulation areas, which then infiltrates into blocky, highly conductive colluvium further downslope. Surface flow resurfaces in the mainstream or just before entering the mainstream. By contrast, once surface flow initiates along the channels of Cougar, Goat, or Dunce watersheds, it is more likely to remain at the surface. We hypothesize that these differences are primarily because of different weathering characteristics of Pioneer watershed's quartzite and metasedimentary rocks compared with the granodiorite that dominates the terrain north of Big Creek (i.e. Cougar, Goat, and Dunce watersheds) (Figures 9 and 4). We observed that the quartzite and other metasedimentary rocks of Pioneer watershed break into large blocks and cobbles that collect in valley bottoms (Figure 9A). Flow likely encounters this thickening layer of conductive blocky debris, and rapidly infiltrates until that layer shallows to a point less than the thickness of the saturated debris, or to a point when there is enough water to transport the debris. In Pioneer watershed, there are numerous locations where there is insufficient water to erode a deep channel through the valley-bottom blocky debris until the main channel. Conversely, in Cougar, Goat, and Dunce watersheds, we observed that the granodiorite generally weathers into a finer, sandy grus. This smaller material is more easily transported, and thus, stream channels are initiated and maintained throughout greater extents of these watersheds (Figure 9B).

Our observations of different weathering characteristics in the lower Big Creek watersheds are consistent with

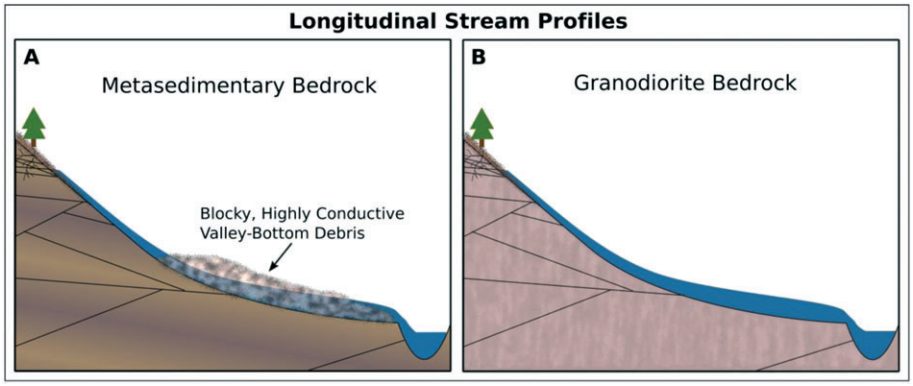


Figure 9. (A) The metasedimentary rock the predominantly underlies Pioneer watershed weathers into large blocks and cobbles that collect in valley bottoms. Streams will infiltrate into this highly conductive debris until water depth is greater than debris thickness. (B) The granodiorite that predominantly underlies Cougar, Goat, and Dunce watersheds weathers into a sandy grus, which smaller streams are more capable of transporting. Thus, streamflow through granodiorite is more continuous

well-weathered granites observed by Rugenski and Minshall (2014) in the same study area. It is also likely that fracture and joint geometries differ within granodiorite and the metasedimentary units. This would influence deeper flowpath and storage characteristics potentially resulting in differences in active drainage network response to discharge.

Suspended sediment and bedload transport analyses may help quantify the differences of bedrock weathering and channel development within metasedimentary *versus* granodioritic bedrock. Also, green light detection and ranging that penetrates water would allow for more detailed analysis of difference between channel geometries. It is likely that in granodiorite-dominated areas, smaller fluvial channels will be detectable, while in areas underlain by metasedimentary rocks, channel development will only occur at larger scales where flows are great enough to transport large debris.

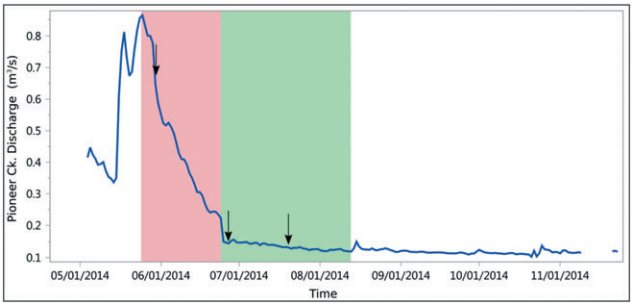


Figure 10. Pioneer Creek hydrograph. The rapid recession period (red) extends from 25 May 2014 to 24 June 2014, followed by a more gradual asymptotic recession (green). The rapid recession has a log-log slope of $-1.63$ ($R^2 = 0.98$, $p < 0.0001$), and the asymptotic recession from 25 June 2014 to 13 August 2014 has a log-log slope of $-0.39$ ($R^2 = 0.92$, $p < 0.0001$). Arrows indicate the three active drainage network surveys of Pioneer Creek on 28–31 May 2014, 25–27 June 2014, and 18–20 July 2014

*Streamflow recession*

High-elevation snowpacks in the lower Big Creek watersheds typically persist for more than 180 days in an average year (Tennant *et al.*, 2015). The mountains then shed this stored water during the spring and early summer melt. In 2014, after snowmelt-induced peak flows, an approximately 28-day period of rapid recession at Pioneer Creek transitioned to an asymptotic recession (Figure 10). Pioneer watershed releases most of its water roughly six times faster than it accumulates as autumn and winter snowpacks; it releases the melt via short, fast, and shallow flow paths through thin soil and colluvium layers. The onset of the asymptotic flow recession at the beginning of July suggests the transition to deeper groundwater (bedrock aquifer) dependent baseflows with very little excess shallow water entering the stream from the highly conductive soil and debris layers. Low-flow conditions initiated towards the beginning of July and persisted until the end of the study period.

## CONCLUSIONS

In Pioneer Creek, and many other streams of western North America, streamflow generated by spring snowmelt is much greater than baseflow conditions during the rest of the annual hydrograph. However, the observed active drainage networks do not exhibit the same degree of fluctuation. Shaw (2015) observed that streamflow recedes at a different rate than the rate at which the active drainage network shortens, consistent with a non-linear relationship between network length and flow. We also observed more stability in the active drainage network than in streamflow during the seasonal snowmelt recession.

We observed that the majority of flowheads are stable. Stable flowheads with large accumulation areas on

 

concave slopes are likely supported by converging, long, slow and deep flowpaths. At our study sites, the 21% of flowheads that are unstable are primarily on south- to southwest-facing, high-elevation, planar slopes with small accumulation areas where parallel, short, fast, and shallow flowpaths predominate. That is, active drainage networks are mostly fed by flowpaths through bedrock aquifers, and only partially via fast, ephemeral and shallow snowmelt drainage through conductive soil and colluvium layers. These faster flowpaths are reflected by surface topography (i.e. accumulation area, concavity, elevation, and aspect), so flowhead stability sometimes correlates with topographic characteristics.

Our work suggests that connections and disconnections along the active drainage network reflect different weathering characteristics of underlying geology. In our study area, the active drainage network of Pioneer Creek is more sensitive to changes in discharge than other sites, which is likely because of flow infiltrating downslope accumulations of largely immobile metasedimentary cobbles and boulders. Conversely, the granodiorite underlying Cougar, Goat, and Dunce Creeks weathers to a more easily transported sandy grus, resulting in more continuous channels.

Field observations of the active drainage network emphasize more complex spatial processes than are often represented in models, with potential limitations of watershed-scale storage-discharge relationships (e.g. Biswal and Marani, 2010; Kirchner 2009). Isotopic and other chemical analyses of flowhead water (e.g. Mueller *et al*., 2014; Liu *et al*., 2013; Zimmer *et al*., 2013) across elevations and network stability gradients would identify the sources and ages of water supporting surface flow. Geophysical mapping upslope of flowheads could provide imagery of bedrock topography and structure. These analyses could further explore the linkages between greater flowhead stability and long, slow, bedrock flowpaths.

If active drainage network dynamics reliably reflect flowpath characteristics, repeated surveys over different flow conditions may be an important tool in accessing stream susceptibility to climate change. As increasing amounts of precipitation fall as rain instead of snow in mountainous watersheds of western North America, long-term studies may reveal shifts in dominant flowpath dynamics with important implications for surface water hydrology, stream chemistry, and ecology.

## ACKNOWLEDGEMENTS

We thank the Gäg Family for their support as managers of the University of Idaho Taylor Wilderness Research Station. G. Thackray, K. Reinhardt, B. Crosby, and C. Tennant provided helpful advice and discussion, and C. Bottenberg provided GIS assistance. This work was supported by Sigma Xi, the Geslin Fund, NSF EPSCoR WRCC, Idaho State University, and especially, the DeVlieg Foundation.

## REFERENCES

Anderson RS, Anderson SP, Tucker GE. 2013. Rock damage and regolith transport by frost: an example of climate modulation of the geomorphology of the critical zone. *Earth Surface Processes and Landforms* **38**(3): 299–316. DOI:10.1002/esp.3330.

Bencala KE, Gooseff MN, Kimball BA. 2011. Rethinking hyporheic flow and transient storage to advance understanding of stream-catchment connections. *Water Resources Research* **47**(3): W00H03. DOI:10.1029/2010WR010066.

Bièvre G, Jongmans D, Winiarski T, Zumbo V. 2012. Application of geophysical measurements for assessing the role of fissures in water infiltration within a clay landslide (Trièves area, French Alps). *Hydrological Processes* **26**(14): 2128–2142. DOI:10.1002/hyp.7986.

Bishop K, Buffam I, Erlandsson M, Fölster J, Laudon H, Seibert J, Temnerud J. 2008. Aqua Incognita: the unknown headwaters. *Hydrological Processes* **22**(8): 1239–1242. DOI:10.1002/hyp.7049.

Biswal B, Marani M. 2010. Geomorphological origin of recession curves. *Geophysical Research Letters* **37**(24): . DOI:10.1029/2010GL045415.

Biswal B, Nagesh KD. 2013. A general geomorphological recession flow model for river basins. *Water Resources Research* **49**(8): 4900–4906. DOI:10.1002/wrcr.20379.

Blyth K, Rodda J. 1973. A stream length study. *Water Resources Research* **9**(5): 1454–1461. DOI:10.1029/WR009i005p01454.

Buttle JM, Dillon PJ, Eerkes GR. 2004. Hydrologic coupling of slopes, riparian zones and streams: an example from the Canadian Shield. *Journal of Hydrology* **287**(1–4): 161–177. DOI:10.1016/j.jhydrol.2003.09.022.

Colman SM, Pierce KL. 1986. Glacial sequence near McCall, Idaho: weathering rinds, soil development, morphology, and other relative-age criteria. *Quaternary Research* **25**(1): 25–42. DOI:10.1016/0033-5894(86)90041-4.

Daesslé LW, Pérez-Flores MA, Serrano-Ortiz J, Mendoza-Espinosa L, Manjarrez-Masuda E, Lugo-Ibarra KC, Gómez-Treviño E. 2014. A geochemical and 3D geometry geophysical survey to assess artificial groundwater recharge potential in the Pacific coast of Baja California, Mexico. *Environmental Earth Sciences* **71**(8): 3477–3490. DOI:10.1007/s12665-013-2737-9.

Davis JM, Baxter CV, Minshall GW, Olson NF, Tang C, Crosby BT. 2013. Climate-induced shift in hydrological regime alters basal resource dynamics in a wilderness river ecosystem. *Freshwater Biology* **58**(2): 306–319. DOI:10.1111/fwb.12059.

Day DG. 1978. Drainage density changes during rainfall. *Earth Surface Processes* **3**(3): 319–326. DOI:10.1002/esp.3290030310.

Day DG. 1983. Drainage density variability and drainage basin outputs (New South Wales, Australia). *Journal of Hydrology. New Zealand* **22**: 3–17.

Dingler CM, Breckenridge RM. 1982. Glacial reconnaissance of the Selway-Bitterroot Wilderness Area, Idaho. In *Cenozoic Geology of Idaho*, Bonnichsen B, Breckenridge RM (eds). Idaho Bureau of Mines and Geology: Moscow, Idaho; 645–652.

Evenson EB, Cotter JFP, Clinch JM. 1982. Glaciation of the Pioneer Mountains: a proposed model for Idaho. In *Cenozoic Geology of Idaho*, Bonnichsen B, Breckenridge RM (eds). Idaho Bureau of Mines and Geology: Moscow, Idaho; 645–652.

Freer J, McDonnell JJ, Beven KJ, Peters NE, Burns DA, Hooper RP, Aulenbach B, Kendall C. 2002. The role of bedrock topography on subsurface storm flow. *Water Resources Research* **38**(12): 5–1–5–16. DOI: 10.1029/2001WR000872

Gabrielli CP, McDonnell JJ, Jarvis WT. 2012. The role of bedrock groundwater in rainfall-runoff response at hillslope and catchment scales. *Journal of Hydrology* **450–451**: 117–133. DOI:10.1016/j.jhydrol.2012.05.023.

Gannon J, Bailey S, McGuire K. 2014. Organizing groundwater regimes and response thresholds by soils: a framework for understanding runoff

 

generation in a headwater catchment. *Water Resources Research* **50** (11): 8403–8419. DOI:10.1002/2014WR015498.

Godsey SE, Kirchner JW. 2014. Dynamic, discontinuous stream networks: hydrologically driven variations in active drainage density, flowing channels and stream order. *Hydrological Processes* **28**(23): 5791–580. DOI:10.1002/hyp.10310.

Goyal MK, Madramootoo CA, Richards JF. 2015. Simulation of the streamflow for the Rio Nuevo Watershed of Jamaica for use in agriculture water scarcity planning. *Journal of Irrigation and Drainage Engineering* **141**(3): 04014056. DOI:10.1061/(ASCE)IR.1943-4774.00008022.

Gregory KJ, Walling DE. 1968. The variation of drainage density within a catchment. *International Association of Scientific Hydrology Bulletin* **13** (2): 61–68. DOI:10.1080/02626666809493583.

Hinckley ELS, Ebel BA, Barnes RT, Anderson RS, Williams MW, Anderson SP. 2014. Aspect control of water movement on hillslopes near the rain-snow transition of the Colorado Front Range. *Hydrological Processes* **28** (1): 74–85. DOI:10.1002/hyp.9549.

Jaeger KL, Olden JD, Pelland NA. 2014. Climate change poised to threaten hydrologic connectivity and endemic fishes in dryland streams. *Proceedings of the National Academy of Sciences of the United States of America* **111**(38): 13894–13899. DOI:10.1073/pnas.1320890111.

Kirchner JW. 2009. Catchments as simple dynamical systems: catchment characterization, rainfall-runoff modeling, and doing hydrology backward. *Water Resources Research* **45**(2): W02429. DOI:10.1029/2008WR006912.

Kirchner JW, Finkel RC, Riebe CS, Granger DE, Clayton JL, King JG, Megahan WF. 2001. Mountain erosion over 10 yr, 10 ky, and 10 my time scales. *Geology* **29**(7): 591–594. DOI:10.1130/0091-7613(2001)029<0591:MEOYKY>2.0.CO.

Knowles N, Dettinger M, Cayan D. 2006. Trends in snowfall versus rainfall in the western United States. *Journal of Climate* **19**(18): 4545–4559. DOI:10.1175/JCLI3850.1.

Leopold LB, Wolman MG, Miller JP. 1964. *Fluvial Processes in Geomorphology*. W.H. Freeman and Company: San Francisco; 522.

Lifton ZM, Thackray GD, Van Kirk R, Glenn NF. 2009. Influence of rock strength on the valley morphometry of Big Creek, central Idaho, USA. *Geomorphology* **111**(3–4): 173–181.DOI:10.1016/j.geomorph.2009.04.014.

Link PK, Crosby BT, Lifton ZM, Eversole EA, Rittenour TM. 2014. The late Pleistocene (17 ka) Soldier Bar landslide and Big Creek Lake, Frank Church-River of No Return Wilderness, central Idaho, U.S.A. *Rocky Mountain Geology* **4**(1): 17–31.

Liu F, Hunsaker C, Bales RC. 2013. Controls of streamflow generation in small catchments across the snow-rain transition in the Southern Sierra Nevada, California. *Hydrological Processes* **27**(14): 1959–1972. DOI:10.1002/hyp.9304.

Lundeen KA. 2001. Refined late Pleistocene glacial chronology for the eastern Sawtooth Mountains, central Idaho [Master's thesis]: Pocatello, Idaho, Idaho State University, 58 p.

Manning AH, Clark JF, Diaz SH, Rademacher LK, Earman S, Niel PL. 2012. Evolution of groundwater age in a mountain watershed over a period of thirteen years. *Journal of Hydrology* **460-461**: 13–28. DOI:10.1016/j.jhydrol.2012.06.030.

McNamara JP, Tetzlaff D, Bishop K, Soulsby C, Seyfried M, Peters NE, Hooper R. 2011. Storage as a metric of catchment comparison. *Hydrological Processes* **25**(21): 3364–3371. DOI:10.1002/hyp.8113.

Meyer GA, Leidecker ME. 1999. Fluvial terraces along the middle fork Salmon River, Idaho and their relation to glaciation, landslide dams, and incision rates: a preliminary analysis and river-mile guide: a preliminary analysis and river-mile guide. In *Guidebook to the Geology of Eastern Idaho*, Hughes SS, Thackray GD (eds). Idaho Museum of Natural History: Pocatello, Idaho; 219–235.

Mueller MH, Alaoui A, Kuells C, Leistert H, Meusburger K, Stumpp C, Weiler M, Alewell C. 2014. Tracking water pathways in steep hillslopes by $\delta^{18}O$ depth profiles of soil water. *Journal of Hydrology* **519**: 340–352.

Rademacher LK, Clark JF, Clow DW, Hudson GB. 2005. Old groundwater influence on stream hydrochemistry and catchment response times in a small Sierra Nevada catchment: Sagehen Creek, California. *Water Resources Research* **41**(2): 1–10. DOI:10.1029/2003WR002805.

Roberts MC, Archibold OW. 1978. Variation of drainage density in a small British Columbia watershed. *AWRA Water Resources Bulletin* **14** (2): 470–476. DOI:10.1111/j.1752-1688.1978.tb02183.x.

Roberts M, Klingeman P. 1972. The relationship between drainage net fluctuation and discharge. In *International Geography, Proceedings of the 22nd International Geographical Congress, Canada*, Adams, Helleiner (eds). University of Toronto Press: Toronto, Ontario, Canada; 189–191.

Rugenski AT, Minshall GW. 2014. Climate-moderated responses to wildfire by macroinvertebrates and basal food resources in montane wilderness streams. *Ecosphere* **5**(3): 25. DOI:10.1890/ES13-00236.1.

Shaw SB. 2015. Investigating the linkage between streamflow recession rates and channel network contraction in a mesoscale catchment in New York State. *Hydrological Processes* **63**(3): . DOI:10.1002/hyp.10626.

Stewart DE, Lewis RS, Stewart ED, Link PK. 2013. Geologic map of the central and lower Big Creek drainage, central Idaho: Idaho Geological Survey Digital Web Map, scale 1:75,000.

Stewart I, Cayan D, Dettinger M. 2004. Changes in snowmelt runoff timing in Western North America under a "business as usual" climate change scenario. *Climatic Change* **62**: 217–232.

Sweetkind DS, Blackwell DD. 1989. Fission-track evidence of the Cenozoic thermal history of the Idaho Batholith. *Tectonophysics* **157** (4): 241–250.DOI:10.1016/0040 1951(89)90142-X.

Tennant CJ, Crosby BT, Godsey SE. 2015. Elevation-dependent responses of streamflow to climate warming. *Hydrological Processes* **29**(2015): 991–1001. DOI:10.1002/hyp.10203.

Thackray GD, Lundeen KA, Borgert JA. 2004. Latest Pleistocene alpine glacier advances in the Sawtooth Mountains, Idaho, USA: reflections of midlatitude moisture transport at the close of the last glaciation. *Geology* **32**(3): 225. DOI:10.1130/G20174.1.

Tromp-Van Meerveld HJ, McDonnell JJ. 2006. Threshold relations in subsurface stormflow: 2. The fill and spill hypothesis. *Water Resources Research* **42**(2): . DOI:10.1029/2004WR003800.

U.S. Geological Survey (U.S.G.S). 2014. The StreamStats program for Idaho, online at http://water.usgs.gov/osw/streamstats/idaho.html.

Wagner MJ, Bladon KD, Silins U, Williams CHS, Martens AM, Boon S, MacDonald RJ, Stone M, Emelko MB, Anderson A. 2014. Catchment-scale stream temperature response to land disturbance by wildfire governed by surface-subsurface energy exchange and atmospheric controls. *Journal of Hydrology* **517**: 328–338. DOI:10.1016/j.jhydrol.2014.05.006.

Weis PL, Schmitt LJJ, Tuchek ET. 1972. *Mineral Resources of the Salmon River Breaks Primitive Area, Idaho: 1353-C*. U. S. Geological Survey: Washington, D.C.; C17–C18.

Zimmer MA, Bailey SW, McGuire KJ, Bullen TD. 2013. Fine scale variations of surface water chemistry in an ephemeral to perennial drainage network. *Hydrological Processes* **27**(24): 3438–3451. DOI:10.1002/hyp.9449.

 